Article

Journal of
Nanoscience and Nanotechnology
Vol. 16, 1–7, 2016
www.aspbs.com/jnn

Optical Hyperthermia Using Anti-Epidermal Growth Factor Receptor-Conjugated Gold Nanorods to Induce Cell Death in Glioblastoma Cell Lines

Tamara Fernández-Cabada[1], Cristina Sánchez-López de Pablo[1,2], Liudmila Pisarchyk[1], José Javier Serrano-Olmedo[1,2], and Milagros Ramos-Gómez[1,2,*]

[1] *Centre for Biomedical Technology (CTB), Technical University of Madrid (UPM), Madrid, Spain*
[2] *Biomedical Research Networking Center in Bioengineering Biomaterials and Nanomedicine (CIBER-BBN), Madrid, Spains*

Gold nanorods (GNRs) are able to efficiently convert absorbed light into localized heat within a short period of time due to the surface plasmon resonance effect. This property, along with their easy bioconjugation, allows the use of GNRs in photothermal therapy as selective photothermal agents to target cancer cells. In this study, GNRs were combined with an antibody against anti-epidermal growth factor receptor (EGFR), a receptor that is frequently overexpressed in brain tumors, and the potential of the nanoconjugate (EGFR-GNRs) to eliminate tumor cells was assessed *in vitro*. Two human glioblastoma cell lines (U373-MG and 1321N1) expressing EGFR at different levels were incubated with unfunctionalized GNRs and EGFR-GNRs, and then exposed to irradiation with a continuous-wave laser at 808 nm. The pretreatment with the EGFR-GNR nanoconjugate significantly increased the cell death rate after laser irradiation compared to unconjugated GNRs. No photothermal cell destruction was observed in the absence of GNRs. Our data suggest that the EGFR modification improves GNR-mediated cell death after laser irradiation, even when EGFR is present at low doses in cancer cells, and may have the potential to be used clinically as a tool to help complete resection of brain tumors during surgery.

Keywords: Gold Nanorods, EGFR, Optical Hyperthermia, Biofunctionalization, Glioblastoma Cell Lines.

1. INTRODUCTION

Glioblastoma multiforme (GBM) is the most common and deadliest form of malignant primary brain tumors in adults.[1] GBM are usually highly malignant because tumor cells, with both oligodendroglial and astrocytic components, proliferate quickly and are supported by a large network of blood vessels.[2] The World Health Organization has classified GBM as a class IV malignancy.[3] This classification refers to the tumors high rate of proliferation, increased angiogenesis, invasiveness into the surrounding tissues, and fatal outcome. The poor prognosis associated with GBM is a direct effect of the tumors diffuse proliferation, along with its resistance to traditional treatments.[4–7]

Current standard therapy for GBM consists of surgery followed by radiotherapy combined with chemotherapy. Studies have shown that near-complete tumor resection improves patient prognosis by preventing tumor recurrence and by avoiding the need for a second surgery. However, achieving a maximal extent of resection can be quite difficult due to the invasive nature of the tumor. Therefore, the complete success of tumor removal requires the development of new effective therapies for the total elimination of invasive tumor cells.[8]

Hyperthermia is a noninvasive anticancer approach in which biological tissues are exposed to temperatures higher than normal (41–47 °C) to promote selective destruction of abnormal cells.[9] Because of their poor vascular network and reduced heat tolerance, tumors are selectively destroyed in this temperature range. Thus, hyperthermia for anticancer treatment could inhibit tumor cell proliferation by destroying cancer cells or by making them more sensitive to the effects of conventional antitumor therapies, such as radiation or chemotherapy.[9]

Gold nanoparticles, in combination with laser light, have been used successfully to achieve controlled thermal

*Author to whom correspondence should be addressed.

damage in tumor tissue.[10–12] Gold nanostructures possess a unique optical property: they strongly absorb light due to surface plasmon resonance converting absorbed light into localized heat.[13, 14] This strategy has been used to develop thermotherapy for cancer treatment. More specifically, gold nanorods (GNRs) are of special interest because they have large light-absorption cross-sections. GNRs exhibit two distinct surface plasmon oscillations: the longitudinal band, a strong band in the near-infrared region, and the transverse band, a weak band in the visible region.[13] Only the longitudinal band is sensitive to size changes, and can be shifted from visible to near-infrared by adjusting the aspect ratio (length/width) during the process of synthesis.[13]

In addition, GNRs have shown a good biocompatibility[12] and quick clearance in blood, while exhibiting longer retention times in tissues such as liver, spleen and kidneys.[15, 16]

The biofunctionalization of GNRs with molecules to target cancer cells has proven highly effective. GNRs have been conjugated to antibodies to specifically target and destroy different types of human carcinomas.[17, 18] The biofunctionalization results in accumulation of GNRs on the cell surface, rendering the tumor cells highly susceptible to photothermal damage.[10]

Epidermal growth factor receptors (EGFRs), also known as ErbB receptors, are often overexpressed on cancer cell surfaces and can lead to activation of multiple pathways linked to malignancy.[19] EGFR overexpression is linked to recurrent and high-risk cases in multiple types of cancer.[20, 21] Therefore, EGFRs are important diagnostic markers and targets for therapeutic intervention.[22] Approximately 40–50% of GBM tumors contain amplifications of the wild-type EGFR gene, making EGFR overexpression the most common mutation in GBMs.[6, 23, 24] Therefore, EGFR can be proposed as an effective target for molecular labeling of GBMs.

This article describes the advantages of using EGFR-biofunctionalized GNRs versus unfunctionalized GNRs to achieve better results in eliminating tumor cells by photothermal therapy.

2. EXPERIMENTAL DETAILS

2.1. Optical Hyperthermia Device

The continuous wave laser (MDL H808, PSU-H-LED power source; Changchung New Industries, Changchun Jilin, China) works at 808 nm, with a maximum output power of 5 W, a beam height from base of 29 mm, a beam diameter with an aperture of 5–8 mm^3, and laser head dimensions of $155 \times 77 \times 60$ mm^3. GNRs (10×43 nm; PEG-10-808-100, NanoSeedzTM, OD/ml: 10) were tuned to the laser source, with a surface plasmon resonance peak (longitudinal band) at 808 nm. Temperature control was achieved using a precision thermometer (F100; Automatic Systems Laboratories, Redhill, UK). The laser was connected to the system via a multimode optical fiber with a core diameter of 600 μm, a length of 1.5 m, and a power transmission of 90–99% (600 μm MM fiber; Changchung New Industries). The optical fiber was fixed to the lower region of the well irradiating the samples through a collimating lens (78382; Newport, Irvine, CA) for a period of 40 and 75 min at 2.5 W/cm^2.

2.2. Preparation of Anti-EGFR Antibody-Conjugated Gold Nanorods

The anti-EGFR-GNR conjugates were prepared according to a modification of the method described by Sokolov.[25] Briefly, the gold nanorods were washed in H_2O and diluted in 20 mM HEPES buffer (pH 7.4) to a final concentration 0.6 mg/ml. The polyclonal antibody anti-EGFR (30 μg/ml; Abcam) and polyethyleneglycol to prevent aggregation (5 mg/ml; Sigma) were added. The solution was mixed for 48 h at room temperature, centrifuged at 6000 rpm for 18 min and the pellet was resuspended in 1 ml PBS buffer (pH 7.4). The solution was centrifuged again for 18 minutes at 6000 rpm and redispersed in Dulbeccós modified Eaglés medium supplemented with 5% heat-inactivated fetal bovine serum, 2 mM L-glutamine, 100 U/ml penicillin and 100 μg/ml streptomycin (Life Technologies, Grand Island, NY).

2.3. Dot-Blot and Bradford Protein Assay

To test the efficiency of the coupling reaction of the anti-EGFR antibody to the GNRs, 1 μl drops of each solution used in the preparation of the EGFR-GNR conjugate (anti-EGFR antibody, GNRs alone, medium containing unbound anti-EGFR antibody, and EGFR-GNR conjugate) were deposited onto a nitrocellulose membrane strip (Bio-Rad). After drying at room temperature, dot-blots were first blocked for 1 h at room temperature with 5% skim milk in Tris-buffered saline (500 mM NaCl in 20 mM Tris, pH 7.4) containing 0.05% Tween 20 (TTBS), and then incubated for 1 h with a goat anti-rabbit-peroxidase conjugate antibody (1:5000; Life Technologies). Immunoreactivity was detected using the ECL Western blotting detection system (Amersham Biosciences). In addition, protein concentrations in coupling reaction (total and unbound antibody) were determined by an improved Bradford protein assay permitting quantification of low protein concentrations,[26] in order to confirm dot blot results. The binding efficiency was calculated as previously described in Ref. [27] resulting to be about 90% and 11.5+/−4 molecules of anti-EGFR bound per nanoparticle.

2.4. Cell Cultures

Human brain astrocytoma cell lines (U373-MG; ECACC 89081403, and 1321N1; ECACC 86030402) were maintained in Dulbeccós modified Eaglés medium supplemented with 10% heat-inactivated fetal bovine serum, 2 mM L-glutamine, 100 U/ml penicillin, and 100 μg/ml streptomycin (Life Technologies, Grand Island, NY). The

cell lines were maintained at 37 °C in 5% CO_2 and 95% air in a humidified atmosphere and passaged twice a week.

2.5. Western Blotting

1321N1 and U373-MG cell lines were harvested using trypsin/EDTA (Invitrogen), washed twice with PBS, and resuspended in lysis buffer (1% Triton X-100, 150 mM NaCl, 20 mM Tris-HCl, pH 7.5, 0.5 mM EDTA, 1 mM EGTA) in the presence of protease inhibitors (complete mini-EDTA-free protease inhibitor mixture tablets, Roche Applied Science) for 30 min at 4 °C and centrifuged at maximum speed for 20 min at 4 °C. Protein concentration in the supernatants was determined using the Bradford protein assay (Bio-Rad). Proteins (25 μg) were separated in a 8% SDS-polyacrylamide gel and transferred to a nitrocellulose membrane. Blots were then incubated overnight at 4 °C with monoclonal antibodies against β-actin (1:5000; Sigma) or rabbit polyclonal anti-EGFR antibody (1:200; Abcam). Secondary antibodies were used at 1:10,000 (Bio-Rad) for peroxidase anti-mouse antibody and 1:3000 for peroxidase anti-rabbit antibody (Vector). Immunoreactivity was detected using the ECL Western blotting detection system (Amersham Biosciences).

2.6. Immunocytochemistry

Cells were fixed in 4% paraformaldehyde in phosphate buffer (pH 7.5), blocked for 1 h in 10% normal goat serum in TTBS, and incubated overnight at 4 °C with an anti-EGFR antibody (1:40, Abcam) followed by incubation with a biotinylated goat anti-rabbit IgG antibody (1:100, Vector Labs) and fluorescein streptavidin (excitation 495 nm; emission 515 nm, 1:300, Vector Labs) for 1 h. Cell nuclei were counterstained with Hoechst 33258 (0.2 mg/ml; Molecular Probes, Eugene, OR). Images were captured using a Leica DMIRB microscope equipped with a digital camera Leica DC100 (Nussloch, Germany).

2.7. Confocal Laser Scanning Microscopy

For phase-contrast microscopy observations, an initial density of 5×10^4 cells/cm^2 was seeded in 0.5 ml of cell culture medium onto glass coverslips in 24-well plates and allowed to grow for 24 h prior to adding GNRs and EGFR-GNR conjugates at 0.06 mg/ml. After 75 min of incubation in the presence of GNRs, the medium was removed, and the cells were washed twice with phosphate-buffered saline solution, and fixed in 4% paraformaldehyde. Cells were stained with phalloidin (1:500, Sigma) to visualize the cytoskeleton, and then incubated with goat anti-rabbit FITC-conjugated antibody (1:300, Jackson Immunoresearch) to detect EGFR-GNRs. Cell nuclei were counterstained with ToPro (1:500, Invitrogen). GNRs were detected by reflection under excitation with a laser of 488 nm and by collecting the emission in the 426–446 nm range. Images were captured using a Zeiss LSM510 confocal microscope.

2.8. Total-Reflection X-ray Fluorescence (TXRF) Spectrometry

To determine the affinity of EGFR-GNRs for U373-MG and 1321N1 cells, Au ion concentration was assessed by TXRF, as previously described in Ref. [16]. To this end, U373-MG and 13121N1 cells (2.5×10^5 cells/ml) were incubated with GNRs and EGFR-GNRs at 0.06 mg/ml for 75 min. Cells were then washed three times with PBS to remove unbound GNRs. Before the element analysis, cells were detached using trypsin and dissolved in aqua regia for 12 hours at 120 °C. The amount of Au ion isolated in the cells was measured using TXRF.[16]

2.9. Transmission Electron Microscopy (TEM)

U373-MG cells were seeded (2.5×10^5 cells/ml) into 6-well plates. After incubation with GNRs and EGFR-GNRs (0.06 mg/ml) for 12 hours, the medium was removed, and cells washed with PBS 1× solution. Cells were fixed in 4% paraformaldehyde and 2% glutaraldehyde in phosphate buffer 0.1 M, pH 7.4 for 2 hours. Cells were then scraped from the culture dish and centrifuged at 1500 rpm for 5 minutes; the supernatant was removed. Cell pellets were embedded in Epon Araldite resin (polymerization at 65 °C for 15 hours). Thin sections (70 nm) containing the cells incubated with GNRs were placed on the grids and stained for 1 minute, each with 4% uranyl acetate (1:1, acetone: water) and 0.2% Raynolds lead citrate (water), and air-dried. Images were obtained with a JEOL JEM1010 transmission electron microscope.

2.10. Cell Viability After Hyperthermia Treatments

U373-MG and 1321N1 cells (5×10^4 cells/cm^2) were seeded in 24-well plates in 0.5 ml of cell culture medium and allowed to grow for 24 h prior to adding GNRs and EGFR-GNRs at 0.06 mg/ml for 40 and 75 min. After that time, cells were washed to eliminate excess GNRs, and fresh medium was added. Cells were exposed to laser irradiation at 2.5 W/cm^2 for 40 and 75 min. After laser irradiation, cells were washed in PBS and cultured for 24 h under standard conditions for recovery. For the controls (cells without laser irradiation), cells were incubated in cell culture medium alone and in cell culture medium with 0.06 mg/ml of each type of GNRs for 40 and 75 min. Cell viability was determined by the MTS assay using the CellTiter 96H AQueous One Solution Cell Proliferation Assay kit (Promega) following the manufacturer's instructions.

2.11. Statistical Analysis

Results are shown as the mean ± standard error of the mean of data from three to four experiments. Data were analyzed by single-factor analysis of variance followed by the post

hoc Tukeýs honestly significant difference test. A significance level of $p < 0.05$ was chosen, and Sigmaplot 12.5 Software (Systat Software) was used for all statistical tests.

3. RESULTS AND DISCUSSION

In this study, a general strategy was used to evaluate the efficacy of biofunctionalized GNRs compared to unfunctionalized GNRs in photothermal therapy. To provide clinically relevant anticancer functionality, antibodies against EGFR were selected to target tumor cells, since this receptor is overexpressed in many tumor types.[19–25] The GNRs used in the present study showed a high cytocompatibility and typical accumulation and elimination kinetics after their intravenous administration in mice, as it was previously described.[12, 16] Moreover, when the culture medium was irradiated with laser using the same parameters as in this study, temperatures above 50 °C were obtained in the presence of GNRs and below 39 °C in samples without nanorods.[12]

3.1. Biofunctionalization of Gold Nanorods with Anti-EGFR Antibody

Anti-EGFR antibodies were immobilized onto GNRs as previously described in the methods section. The preparation of gold bioconjugates was based on non-covalent binding of the anti-EGFR antibody at its isoelectric point to GNRs leading to the formation of a very stable complex.[25] The efficiency of the antibody binding to GNRs was determined by a dot-blot assay (Fig. 1(A)). Dot-blot analysis suggested a high level of anti-EGFR binding to GNRs, since only small traces of free anti-EGFR were found in the unbound fraction; a high amount of anti-EGFR antibody present at the beginning of the coupling reaction could be detected conjugated to the GNRs in the GNRs-EGFR fraction after the coupling reaction (Fig. 1(A)). These results were also confirmed by the Bradford protein quantification assay. The binding efficiency was estimated to be about 90% with 11.5 ± 4 molecules of antibody bound per nanorod, as it has been described in more detail in the experimental section.

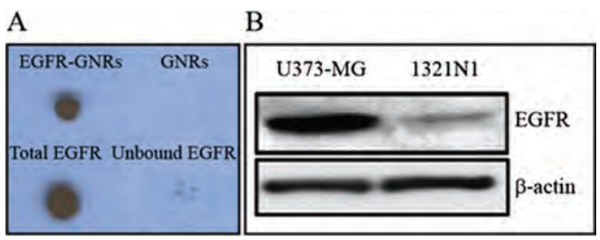

Figure 1. A. Dot-blot assay to determine the effectiveness of EGFR antibody binding to GNRs. One μl of GNRs biofunctionalized with anti-EGFR antibody (EGFR-GNRs), GNRs, EGFR antibody, and unbound fraction from the coupling reaction were placed onto the nitrocellulose membrane. B. Western blot of U3733-MG and 1321N1 cells stained for EGFR and β-actin (used as a loading control).

3.2. Expression of EGFR in Human Glioblastoma Cell Lines

To explore the possibility of EGFR targeting in glioblastoma cell lines, we determined the levels of EGFR expression in two glioblastoma cell lines (U373-MG and 1321N1) by Western blotting (Fig. 1(B)) and immunocytochemistry (Fig. 2). Both cell lines showed EGFR expression at different levels: the U373-MG cell line showed a high EGFR expression while 1321N1 cells exhibited a lower EGFR expression (Figs. 1(B) and 2).

The ability of GNRs conjugated to anti-EGFR antibody to bind to the EGF receptor on the plasma membrane of the two glioblastoma cell lines was assessed by confocal fluorescence microscopy. After exposing U373-MG and 1321N1 cells to anti-EGFR-GNRs for 75 min, the presence of GNRs bound to glioblastoma cells was detected by reflection (blue), and the presence of anti-EGFR antibody bound to GNRs was shown in green by immunofluorescence (Fig. 3).

U373-MG cells (with a high EGFR expression in the plasma membrane) were heavily labeled with EGFR-GNR conjugates (Fig. 3(A)) and easily distinguishable from 1321N1 cells (Fig. 3(B)), which were weakly labeled with the conjugates, since they exhibit a lower expression of EGFR in the plasma membrane. Unfunctionalized GNRs were bound to both glioblastoma cell lines to a much lesser extent than EGFR-GNRs (inserts in Figs. 3(A) and (B), marks in blue). These results were also confirmed by determining the Au ion content in U373-MG and 1321N1 cell lines after incubation with GNRs and EGFR-GNRs for 75 min. TXRF element analysis showed that the number of EGFR-GNRs in both cell lines was higher than that obtained when cells were incubated with unmodified GNRs under the same conditions (Fig. 4(A)). Moreover, cells with a higher EGFR expression (U373-MG cells) showed a higher gold concentration when incubating with EGFR-GNRs (Fig. 4(A)). The results from the TEM observation showed that GNRs (Fig. 4(B)) and EGFR-GNRs (Fig. 4(C)) entered into U373-MG cells after being treated with them for 12 hours. The result indicated that the EGFR-GNRs targeted the EGFR-expressing tumor cells proportionally to their expression levels. In general, the anti-EGFR modification allowed more GNRs to enter both cells; although Au ion can also be detected at lower

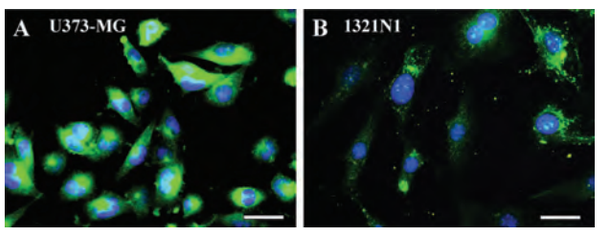

Figure 2. Immunocytochemical staining for EGFR (green) in U373-MG (A) and 1321N1 (B) cell lines. Cell nuclei were counterstained with Hoechst (blue). Scale Bar: 50 μm.

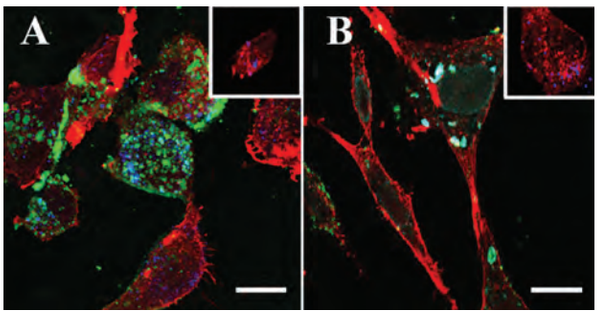

Figure 3. Confocal fluorescence images of U373-MG (A) and 1321N1 (B) cell lines after incubation with EGFR-GNR conjugates. GNRs are shown by laser scanning confocal reflectance in blue. The EGFR antibody conjugated to GNRs was stained in green using an anti-rabbit-FITC antibody. The cellular cytoskeleton was stained with phalloidin (red). Images show higher EGFR-GNR binding to U373-MG (high EGFR expression) cells than to 1321N1 cells (low EGFR expression). Unfunctionalized GNRs exhibited minimal binding to both cell lines (inserts in A and B). Scale bar: 20 μm for all images.

concentrations, in both cell lines when using unmodified GNRs (Fig. 4(A)).

In the present study, we used biofunctionalized EGFR-GNRs as heat-inducing agents under laser radiation in order to obtain a high rate of death of glioblastoma cells. It has been described that many solid tumors (especially glioblastomas) over-express the EGF receptor.[28–30] Therefore; the use of functionalized EGFR-GNRs could promote a selective and localized binding of nanoparticles to tumor cells.

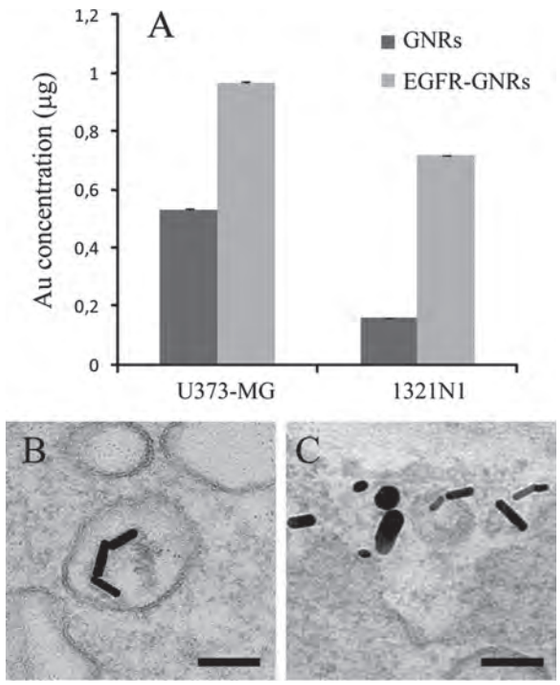

Figure 4. Cellular uptake of GNRs and EGFR-GNRs by U373-MG and 1321N1 cells, Au ion concentration was measured by TXRF after preincubating cells (2×10^5 cells) with gold nanorods at 0.06 mg/ml for 75 min (A). TEM images of U373-MG cells treated with GNRs (B) and EGFR-GNRs (C). Scale bar: 80 nm.

The effectiveness of photothermal therapy has also been described in other tumor cell lines, including human oral epithelial cells,[31] squamous epithelium carcinoma cells,[32] epithelial cervical carcinoma,[33–35] and squamous epithelial cells.[36] Therefore, the use of EGFR expression as a tumor marker and its application in photothermal therapy in combination with GNRs has been widely studied. However, to date there are few studies in which efficient methods based on functionalized GNRs for the effective treatment of glioblastoma have been described. EGFR-GNRs have only been used to spatially delineate human glioblastoma for classifying normal and malignant brain tissue regions.[7]

The different EGFR expression levels observed in the two cell lines analyzed in this study allowed us to determine the effectiveness of GNR biofunctionalization with EGFR to promote cell death after irradiation with a laser.

3.3. Cytotoxicity Induced by Laser Irradiation in the Presence of Anti-EGFR-GNRs and GNRs

The effectiveness of the optical hyperthermia to induce cell death by laser irradiation in the presence of functionalized (EGFR-GNRs) or unfunctionalized (GNRs) GNRs was determined by assessing cell viability. To study cell death in response to the optical laser-induced hyperthermia, U373-MG and 1321N1 cells were incubated for 40 and 75 min with GNRs-EGFR and GNRs. After the incubation period, GNRs-EGFR and GNRs were removed, fresh culture medium was added, and cell viability was analyzed after the irradiation of glioblastoma cell lines with a continuous-wave laser at 2.5 W/cm^2 for 40 min. Increments (Δ) in cell death resulting from the laser irradiation after the preincubation of both cell lines with both types of nanoparticles (functionalized and unfunctionalized) are shown in Figure 5. Only slight increases in cell death rates were observed when cells were irradiated at 2.5 W/cm^2 in the absence of GNRS (Control in Fig. 5), a common range power used in other studies.[37–40] However, this power is higher than the maximal permissible exposure (MPE) of skin per American National Standard for Safe Use of Lasers regulation (0.4 W/cm^2).[41] Therefore, it is highly needed to design more efficient nanomaterials for future *in vivo* applications. When U373-MG cells—which express EGFR at high levels—were incubated with EGFR-GNRs for 40 min and then irradiated, the cells showed a significant increase in cell death compared to cells irradiated in the absence of GNRs. Moreover, when the same cells were incubated with EGFR-GNRs for a longer period of time (75 min), the increase in cell death was significantly different from both cells irradiated without GNRs and cells irradiated with unfunctionalized GNRs (Fig. 4(A)). However, in the 1321N1 cells—which express EGFR at a low level—a significant increase in the percentage of cell death only occurred when cells were preincubated for 75 min with the EGFR-GNRs conjugate (Fig. 4(B)), which is consistent with the decreased expression of the EGF receptor observed in this cell line (Fig. 2(B)).

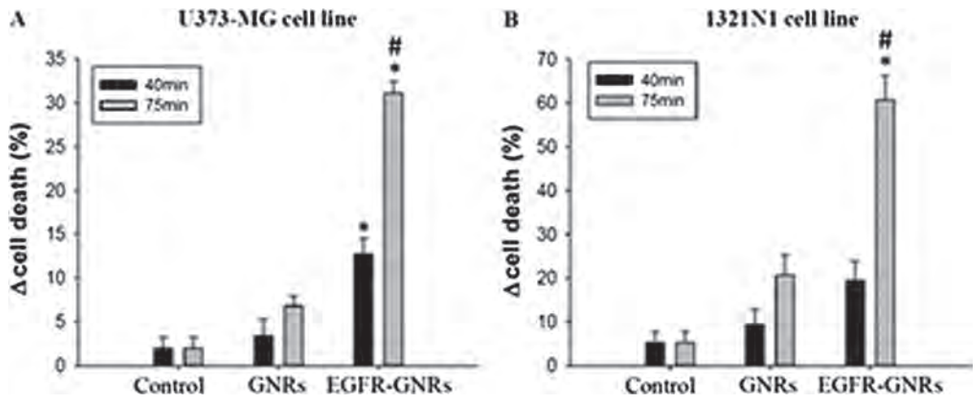

Figure 5. Increase in cell death produced by laser irradiation in U373-MG (A) and 1321N1 (B) cell lines. Cells were incubated with culture medium (Control), unfunctionalized GNRs (GNRs), and GNRs conjugated to anti-EGFR antibodies (GNRs-EGFR) for 40 and 75 min, and were then irradiated with a continuous-wave laser at 5 W for 40 min. Cell viability was assessed by the MTS assay. Specific basal cell death rates for each condition (without laser irradiation) resulted in 17.7+/−1.8% and 18.6+/−1.2% for U373-MG cells incubated with GNRs for 45 and 75 min respectively; 33.2+/−1.8% and 35.7+/−1.1% for U373-MG cells incubated with EGFR-GNRs for 45 and 75 min respectively; 10.1+/−3.7% and 11.2+/−5.2% for 1321N1 cells incubated with GNRs for 45 and 75 min respectively; 20.8+/−4.3% and 17.2+/−6.2% for 1321N1 cells incubated with EGFR-GNRs for 45 and 75 min respectively. Control cells in each cell line were considered as 100% cell viability. Each value represents the mean ± SEM of $n = 3$ independent experiments. ANOVA, Tukey *post hoc*, $^{*}p < 0.05$ compared with cells irradiated without GNRs, $^{\#}p < 0.05$ compared with cells treated with unfunctionalized GNRs.

In photothermal therapy, the biofunctionalization of GNRs with molecules that specifically recognize tumor cells may provide additional support for surgery for complete removal of brain tumors, thus achieving the removal of tumor cells that otherwise would be invisible to surgical resection.

In the cell line that highly expressed EGFR (U373-MG), when cells were irradiated with laser after preincubation with GNRs-EGFR for 40 and 75 min, a statistically significant increase in cell death with respect to cells irradiated in the absence of GNRs occurred; this effect was not achieved when the same cells were incubated with unfunctionalized GNRs. Furthermore, when the cells were preincubated for 75 min with EGFR-GNRs, a significant increase in cell death was observed compared to cells preincubated with unfunctionalized GNRs, demonstrating the significance of an adequate biofunctionalization of the nanorods. In 1321N1 cell line—which showed a lower expression of EGFR than the U373-MG cell line,—when cells were incubated with the EGFR-GNR conjugate for 75 min and subsequently irradiated, a significant increase in cell death compared to both control cells and cells treated with unfunctionalized GNRs occurred. However, in this cell line, no significant increases in cell death rates were obtained when shorter preincubation times with EGFR-GNRs were tested. The difference in the percentage of cell death rates observed in both cell lines might be due to different susceptibilities of the cells in response to an increase in temperature, as we have proved by subjecting the cells to a heat shock (60 °C for 5 min) in a conventional oven. After the heat shock, cell death rates were determined, resulting in 8.03+/−1.83% for U373-MG and 15.68+/−1.00% for 1321N1 cells. However, in both cell lines, the pretreatment with EGFR-GNRs is more effective than using unfunctionalized GNRs to produce cell death after laser irradiation, even in cells with low EGFR expression. The highest absolute cell death rates (65.7% and 77.2% for U373-MG and 1321N1 cells, respectively) were obtained when both cell lines were irradiated after treatment with EGFR-GNRs for 75 min.

4. CONCLUSIONS

The results described here indicate that the biofunctionalization of GNRs with EGFR provides an effective method to induce high mortality rates after laser irradiation in cells expressing EGFR at both high and low concentrations, demonstrating the efficacy of using infrared photothermal therapy to eliminate human glioblastoma cells via biofunctionalized GNRs. These *in vitro* studies have increased the understanding of cellular responses to photothermal therapy, although due to the particular type of cancer, located in the brain, many challenges remain to determine the effects of hyperthermia treatments *in vivo*. Due to the limited capacity of laser penetration in tissues, this method can provide additional aid to surgery to completely remove EGFR-expressing brain tumours using nanoparticles with an appropriate biofunctionalization. This method could thus complete the total removal of the tumor cells that otherwise would be invisible to surgical resection. This combination of active molecular localization and subsequent photothermal treatment of tumor cells may be a feasible application for the treatment of a variety of EGFR-overexpressing tumors, including cervical, colorectal, ovarian, melanoma, lung, pancreas, and prostate cancers.[42–47] In all these types of tumors and due to their anatomical

location, laser irradiation following injection of functionalized GNRs could prevent the need for more invasive treatments, such as surgical resection, and this method may complement methods to achieve complete tumor removal.

Competing Interests

The authors declare that they have no competing interests.

Acknowledgments: The authors would like to thank the expert technical assistance of Soledad Martínez. The authors gratefully acknowledge the financial support of the Reina Sofia Foundation and Comunidad Autónoma Madrid (S2010-BMD-2460) to Milagros Ramos-Gómez and the financial support to Liudmila Pisarchyk by CONACYT (Mexico).

References and Notes

1. T. A. Wilson, M. A. Karajannis, and D. H. Harter, *Surg. Neurol. Int.* 5, 64 (**2014**).
2. A. A. Brandes, A. Tosoni, E. Franceschi, M. Reni, G. Gatta, and C. Vecht, *Crit. Rev. Oncol. Hematol.* 67, 139 (**2008**).
3. D. N. Louis, H. Ohgaki, O. D. Wiestler, W. K. Cavenee, P. C. Burger, A. Jouvet, B. W. Scheithauer, and P. Kleihues, *Acta Neuropathol.* 114, 97 (**2007**).
4. N. R. Smoll, K. Schaller, and O. P. Gautschi, *J. Clin. Neurosci.* 20, 670 (**2013**).
5. P. G. Schmalz, M. J. Shen, and J. K. Park, *Cancers (Basel)* 3, 621 (**2011**).
6. T. Homma, T. Fukushima, S. Vaccarella, Y. Yonekawa, P. L. Di Patre, S. Franceschi, and H. Ohgaki, *J. Neuropathol. Exp. Neurol.* 65, 846 (**2006**).
7. K. Seekell, S. Lewis, C. Wilson, S. Li, G. Grant, and A. Wax, *Biomed. Opt. Express* 4, 2284 (**2013**).
8. G. E. Keles, B. Anderson, and M. S. Berger, *Surg. Neurol.* 52, 371 (**1999**).
9. J. van der Zee, *Ann. Oncol.* 13, 1173 (**2002**).
10. T. B. Huff, L. Tong, Y. Zhao, M. N. Hansen, J. X. Cheng, and A. Wei, *Nanomedicine (Lond).* 2, 125 (**2007**).
11. W. S. Kuo, C. N. Chang, Y. T. Chang, M. H. Yang, Y. H. Chien, S. J. Chen, and C. S. Yeh, *Angew. Chem. Int. Ed. Engl.* 49, 2711 (**2010**).
12. T. Fernandez-Cabada, C. Sanchez Lopez de Pablo, A. Martinez Serrano, F. del Pozo Guerrero, J. J. Serrano Olmedo, and M. Ramos Gomez, *Int. J. Nanomedicine* 7, 1511 (**2012**).
13. X. Huang, P. K. Jain, I. H. El-Sayed, and M. A. El-Sayed, *Lasers Med. Sci.* 23, 217 (**2008**).
14. G. von Maltzahn, J. H. Park, A. Agrawal, N. K. Bandaru, S. K. Das, M. J. Sailor, and S. N. Bhatia, *Cancer Res.* 69, 3892 (**2009**).
15. L. Wang, Y. F. Li, L. Zhou, Y. Liu, L. Meng, K. Zhang, X. Wu, L. Zhang, B. Li, and C. Chen, *Anal. Bioanal. Chem.* 396, 1105 (**2010**).
16. R. Fernández-Ruiz, M. J. Redrejo, E. J. Friedrich, M. Ramos, and T. Fernández-Cabada, *Anal. Chem.* 86, 7383 (**2014**).
17. X. Huang, I. H. El-Sayed, W. Qian, and M. A. El-Sayed, *J. Am. Chem. Soc.* 128, 2115 (**2006**).
18. L. R. Hirsch, R. J. Stafford, J. A. Bankson, S. R. Sershen, B. Rivera, R. E. Price, J. D. Hazle, N. J. Halas, and J. L. West, *Proc. Natl. Acad. Sci. USA.* 100, 13549 (**2003**).
19. C. L. Arteaga and J. A. Engelman, *Cancer Cell* 25, 282 (**2014**).
20. C. R. Leemans, B. J. Braakhuis, and R. H. Brakenhoff, *Nat. Rev. Cancer* 11, 9 (**2011**).
21. I. Vanden Bempt, M. Drijkoningen, and C. De Wolf-Peeters, *Curr. Opin. Oncol.* 19, 552 (**2007**).
22. S. Li, K. R. Schmitz, P. D. Jeffrey, J. J. Wiltzius, P. Kussie, and K. M. Ferguson, *Cancer Cell* 7, 301 (**2005**).
23. H. K. Gan, A. H. Kaye, and R. B. Luwor, *J. Clin. Neurosci.* 16, 748 (**2009**).
24. D. M. Peereboom, D. R. Shepard, M. S. Ahluwalia, C. J. Brewer, N. Agarwal, G. H. Stevens, J. H. Suh, S. A. Toms, M. A. Vogelbaum, R. J. Weil, P. Elson, and G. H. Barnett, *J. Neurooncol.* 98, 93 (**2010**).
25. K. Sokolov, M. Follen, J. Aaron, I. Pavlova, A. Malpica, R. Lotan, and R. Richards-Kortum, *Cancer Res.* 63, 1999 (**2003**).
26. O. Ernst and T. Zor, *J. Vis. Exp.* 38, 1918 (**2010**).
27. S. Charan, K. Sanjiv, N. Singh, F. C. Chien, Y. F. Chen, N. N. Nergui, S. H. Huang, C. W. Kuo, T. C. Lee, and P. Chen, *Bioconjug. Chem.* 23, 2173 (**2012**).
28. N. Shinojima, K. Tada, S. Shiraishi, T. Kamiryo, M. Kochi, H. Nakamura, K. Makino, H. Saya, H. Hirano, J. Kuratsu, K. Oka, Y. Ishimaru, and Y. Ushio, *Cancer Res.* 63, 6962 (**2003**).
29. A. B. Heimberger, D. Suki, D. Yang, W. Shi, and K. Aldape, *J. Transl. Med.* 3, 38 (**2005**).
30. K. J. Hatanpaa, S. Burma, D. Zhao, and A. A. Habib, *Neoplasia.* 12, 675 (**2010**).
31. X. Huang, I. H. El-Sayed, W. Qian, and M. A. El-Sayed, *Nano Lett.* 7, 1591 (**2007**).
32. I. H. El-Sayed, X. Huang, and M. A. El-Sayed, *Cancer Lett.* 239, 129 (**2006**).
33. L. Tong, Y. Zhao, T. B. Huff, M. N. Hansen, A. Wei, and J. X. Cheng, *Adv. Mater.* 19, 3136 (**2007**).
34. H. Takahashi, T. Niidome, A. Nariai, Y. Niidome, and S. Yamada, *Chem. Lett.* 35, 500 (**2006**).
35. Y. Xiao, H. Hong, V. Z. Matson, A. Javadi, W. Xu, Y. Yang, Y. Zhang, J. W. Engle, R. J. Nickles, W. Cai, D. A. Steeber, and S. Gong, *Theranostics* 2, 757 (**2012**).
36. C. S. Rejiya, J. Kumar, V. Raji, M. Vibin, and A. Annie, *Pharmacol. Res.* 65, 261 (**2012**).
37. M. C. Franchini, J. Ponti, R. Lemor, M. Fournelle, F. Broggi, and E. Locatelli, *J. Mater. Chem.* 20, 10908 (**2010**).
38. J. Chen, X. Li, X. Wu, J. T. Pierce, N. Fahruddin, M. Wu, and J. X. Zhao, *Langmuir* 30, 9514 (**2014**).
39. J. Han, J. Li, W. Jia, L. Yao, X. Li, L. Jiang, and Y. Tian, *Int. J. Nanomedicine* 9, 517 (**2014**).
40. S. E. Park, J. Lee, T. Lee, S. B. Bae, B. Kang, Y. M. Huh, S. W. Lee, and S. Haam, *Int. J. Nanomedicine* 10, 261 (**2015**).
41. ANSI, American National Standard for Safe Use of Lasers, Laser Institute of America, Orlando, FL (**2000**).
42. Q. Li, Y. Tang, X. Cheng, J. Ji, J. Zhang, and X. Zhou, *Int. J. Clin. Exp. Pathol.* 7, 733 (**2014**).
43. Q. Y. Feng, Y. Wei, J. W. Chen, W. J. Chang, L. C. Ye, D. X. Zhu, and J. M. Xu, *World J. Gastroenterol.* 20, 4263 (**2014**).
44. J. Eder, I. Simonitsch-Klupp, and F. Trautinger, *Eur. J. Dermatol.* 23, 658 (**2013**).
45. D. Yu, J. Li, Y. Han, S. Liu, N. Xiao, Y. Li, X. Sun, and Z. Liu, *Chin. Med. J. Engl.* 127, 1464 (**2014**).
46. T. Wang, J. Yang, J. Xu, J. Li, Z. Cao, L. Zhou, L. You, H. Shu, Z. Lu, H. Li, M. Li, T. Zhang, and Y. Zhao, *Oncotarget.* 5, 1969 (**2014**).
47. M. Fu, W. Zhang, L. Shan, J. Song, D. Shang, J. Ying, and J. Zhao, *Virchows Arch.* 464, 575 (**2014**).

Received: 1 September 2015. Accepted: 29 October 2015.